The right turn: Modeling driver yielding behavior to e-scooter riders

Citation for the original published paper (version of record):
Rasch, A., Morando, A., Thalya, P. (2025). The right turn: Modeling driver yielding behavior to e-scooter riders. Transportation Research Part F: Traffic Psychology and Behaviour, 115. http://dx.doi.org/10.1016/j.trf.2025.103353

Transportation Research Part F: Psychology and Behaviour 115 (2025) 103353

Contents lists available at ScienceDirect

Transportation Research Part F: Psychology and Behaviour

journal homepage: www.elsevier.com/locate/trf

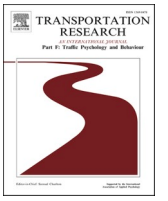

The right turn: Modeling driver yielding behavior to e-scooter riders☆

Alexander Rasch [a,*], Alberto Morando [b], Prateek Thalya [c]

[a] Chalmers University of Technology, Sweden
[b] Autoliv Development AB, Sweden
[c] Magna Electronics Sweden AB, Sweden

ARTICLE INFO

Keywords:
E-scooter
Intersection
Driver behavior
Right turn
Computational model

ABSTRACT

Electric scooters (e-scooters) are a relatively new and popular means of personal transportation in many cities. Notably, they have been involved in crashes with other road users. Crashes with motorized vehicles are particularly critical since they result in more severe injuries or even fatalities. While previous work has highlighted the consequences of failed interactions, we know little about drivers' interactions with e-scooters and how to improve them. In this paper, we conducted a test-track experiment to study how drivers negotiate a right turn at an intersection with an e-scooter. Using Bayesian regression, we modeled whether drivers yield to the e-scooter according to their approaching speed and the difference in time-to-arrival, and we were able to predict drivers' intentions with an AUC of 0.94 and an accuracy of 0.82 in cross-validation. The model coefficients indicate that drivers yield less often when approaching the intersection at a higher speed or larger projected gap. We further modeled drivers' braking timing (time-to-arrival) and strength (mean deceleration), yielding RMSEs of 1.42 s and 0.33 m/s^2, respectively. As a reference for driver behavior when interacting with an e-scooter rider, the model can inform the development and evaluation of support systems to warn drivers more effectively.

1. Introduction

Electric scooters (e-scooters) have become a popular last-mile form of personal transportation (Clough et al., 2023). As the use of e-scooters continues to increase, so do interactions with *motorized vehicles* such as cars, especially in urban areas—where most e-scooters are used (Statistisches Bundesamt, 2022; Wallhagen, 2023). When these interactions fail, they may result in a crash that exposes the e-scooter rider to serious injuries—especially head injuries—often more so than cyclists (Pérez-Zuriaga et al., 2023). Two reasons why e-scooter riders are more vulnerable are the higher travel speed and the critically lower rates of helmet usage (Clough, Platt, Cole, Wilson, & Aylwin, 2023; Stray et al., 2022; Hong et al., 2022).

Severe outcomes of interactions between e-scooters and motorized vehicles are a global phenomenon. For instance, a study in Nashville, Tennessee (US) showed that 80 % of fatal e-scooter crashes involved motorized vehicles (Shah et al., 2021). In 2021 in Germany, 44 % of all e-scooter crashes involving other road users (61 % of all e-scooter crashes) were crashes with passenger cars

☆ This article is part of a special issue entitled: 'Electric personal mobility devices' published in Transportation Research Part F: Psychology and Behaviour.

* Corresponding author.
E-mail address: alexander.rasch@chalmers.se (A. Rasch).

https://doi.org/10.1016/j.trf.2025.103353
Received 31 January 2025; Received in revised form 29 August 2025; Accepted 29 August 2025
Available online 9 September 2025

(Statistisches Bundesamt, 2022). Between 2019 and 2023 in Sweden, collisions with motorized vehicles accounted for the second-most frequent crash scenario (12 % of all crashes) for e-scooter riders (Wallhagen, 2023). Another study from Sweden by Stigson et al. (2024) reported that most of the crashes with passenger cars occurred at intersections when the road-users' paths crossed or the motorized vehicle was making a turn.

The right-turn scenario, in which a driver turns right at an intersection across the path of an approaching vulnerable road user (VRU), is a common crash scenario for both cyclists (Denk et al., 2023; Saul et al., 2021; Schindler & Bianchi Piccinini, 2021) and e-scooter riders (Stigson et al., 2024), who risk being sideswiped by the driver. To avoid a collision, drivers need to slow down and possibly look over their shoulders in a timely manner (Denk et al., 2023). E-scooters are still comparably novel and fast, and their riders often behave more unpredictably (and with smaller safety margins) than cyclists, making their interactions with drivers particularly concerning (Denk et al., 2023; Distefano et al., 2024).

There are multiple ways that the safety of car-to-e-scooter interactions can be improved, such as changes to regulations, infrastructure, and vehicle safety systems. To date, these interactions have been primarily considered to be similar to car-to-cyclist interactions. The Swedish traffic regulation, for example, treats e-scooter riders like bicycle riders and distinguishes between "bicycle crossings" and "bicycle passages". Bicycle crossings are usually elevated and marked with a designated traffic sign, while bicycle passages are only marked with lines on the ground and further subdivided into "supervised" (which are controlled by traffic lights or police officers) and "unsupervised" (which are uncontrolled). At bicycle crossings, *drivers* must give way to bicycle and e-scooter riders. In contrast, at unsupervised bicycle passages, bicycle and e-scooter *riders* must give way to drivers. However, drivers must give riders who are about to enter or are already in the passage an opportunity to cross. Drivers must further maintain a low speed when turning across the passage. This shared responsibility is intended to increase the chances of avoiding a collision (Swedish Transport Agency, 2016).

Vehicle safety systems are intended to avoid or mitigate collisions with VRUs, including e-scooter riders. Advanced driver assistance systems (ADAS), for instance, help avoid collisions by supporting the potentially distracted driver via warnings to help detect the collision threat, or by autonomously braking/steering the vehicle off the collision course (Brännström et al., 2010). Such systems have become increasingly available in consumer vehicles, partly driven by initiatives such as the European New Car Assessment Program (Euro NCAP), which rates vehicles' safety performance and thereby enables consumers to make a safety-driven purchase (Schram et al., 2015). However, the effectiveness of ADAS may be limited by activations perceived as false positives by the driver: if the system issues a warning when the driver is already fully aware of the situation and was planning to react, the driver may lose trust in the system and ignore it or even turn it off. The diminished safety benefit from turning off the system may come at a particularly high cost for VRUs (Lübbe, 2015).

Road-safety initiatives may benefit from detailed knowledge of road-user behavior and reference models. For example, an ADAS may use a driver-behavior model to decide whether the driver is in control of the situation, thereby decreasing the risk of a perceived false positive (Sjöberg et al., 2010). Ljung Aust and Dombrovski (2013) suggested that system activations may be most acceptable when happening outside of the driver's "comfort zone" (i.e., the conditions of driver, vehicle, and environment in which a driver feels at ease). Supporting ADAS with information from a driver model may further enable *earlier* activations (Kovaceva et al., 2022), which is particularly beneficial for VRU safety, since even low impact speeds or close calls may destabilize bicycles/e-scooters and injure the

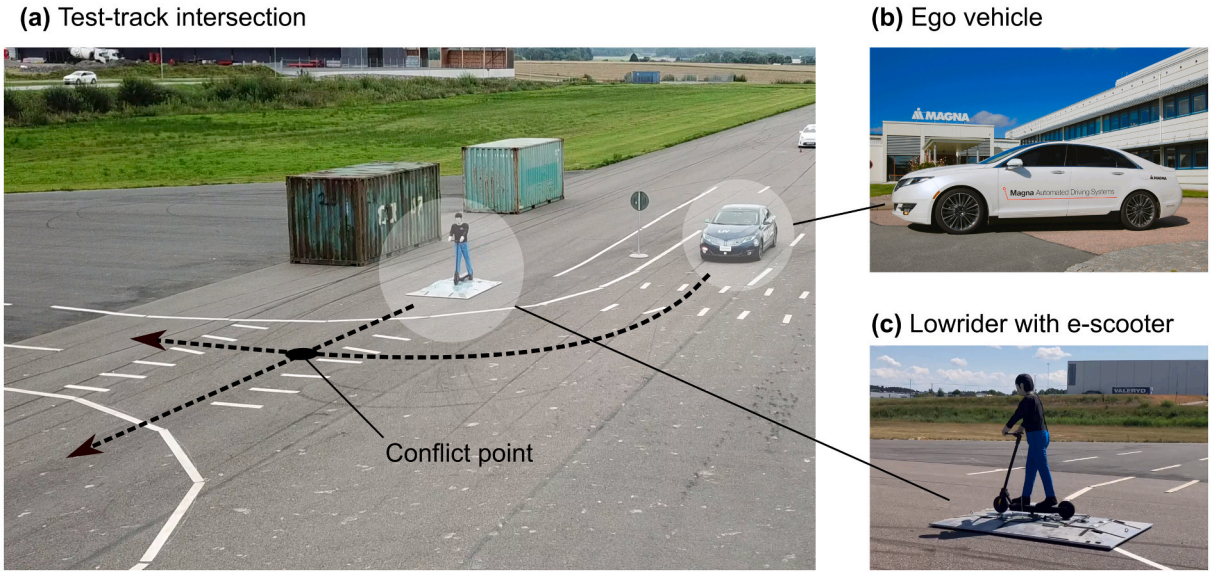

Fig. 1. Test-track experiment at Vårgårda airfield. The intersection is shown in panel a (the photo was taken during a pilot test); panel b shows the ego vehicle, and panel c shows the mobile platform carrying the dummy e-scooter and rider. A video from the pilot test can be found at https://youtu.be/tY1VaxvsVdw.

rider. Unlike bicycles, e-scooters may not be able to self-stabilize (Agúndez et al., 2024) and, therefore, may topple more easily. As a result, it is important to address interactions between drivers and e-scooters specifically in order to improve road safety.

Previous research on e-scooters has documented the consequences of unsafe interactions with drivers. However, we are not aware of any studies that investigated normal behavior, particularly from the driver's perspective, to understand the driver's comfort zone and identify the root causes that may lead to critical events. Notably, we are unaware of prior work attempting to model such interactions computationally. This study aimed to address this gap by providing detailed insights into how drivers negotiate a right turn at an intersection with an e-scooter on a test track. This study also aimed to provide a computational reference model to predict driver behavior in this scenario and discuss how this model can support approaches promoting safer interactions.

2. Method

2.1. Test-track experiment

2.1.1. Experimental protocol

We carried out a test-track experiment in which participants were instructed to drive as they would normally and turn right across a bicycle path at an intersection (Fig. 1). The setting was inspired by the Euro NCAP Car-to-Bicyclist Turning Adult (CBTA) test scenario (Euro NCAP, 2023). The right turns were carried out in eight different combinations of: 1) ego vehicle target speed (30 or 50 km/h), and 2) e-scooter configuration (traveling straight or turning right at the intersection; Fig. 2). The trials in which the e-scooter was turning right were added to reduce the repetitiveness of the experiment and reduce learning effects. The trials in which the e-scooter was traveling straight were repeated three times for each speed, with the car and e-scooter interacting in three specific intended encroachments: 1) ego vehicle crosses first, 2) e-scooter crosses first, and 3) they are on a collision course. The intended encroachments were determined by predicting the path of the ego vehicle and e-scooter based on idealized, assumed speed profiles and delaying the start timing of the e-scooter accordingly. The assumed turning speed for the driver was 10 km/h (in correspondence with the Euro NCAP CBTA scenario), and the assumed braking deceleration was 2 m/s^2. The movement of the e-scooter was predefined and constant; that is, the e-scooter did not slow down or change course even if the car entered the conflict zone (the area where a collision was possible) first. The trials were randomized for each participant to minimize learning effects. Before starting the eight trials, participants completed two training/baseline trials consisting of a right-turn maneuver with the e-scooter stationary in its initial position, at 30 and 50 km/h. After completing all trials, participants were given a questionnaire to capture their experience during the experiment (Fig. A.1 in Appendix A).

2.1.2. Setup

We carried out the experiment during September and October 2023 at Vårgårda Airfield (Vårgårda, Sweden), used as a test track by Magna Electronics. The setup consisted of a straight two-lane road and a side road where the drivers turned right (Fig. 1a). A marked cycle lane next to the road transitioned into an unsupervised bicycle passage that crossed the side road. Containers and a stationary car were placed along the road to increase the scene's realism and improve participants' spatial sense.

Participants drove a Lincoln MKZ 2016 with automatic transmission, referred to as the *ego vehicle* (Fig. 1b). The e-scooter rider was a dummy target from 4activeSystems (Austria), placed on a remote-controlled platform traveling at a constant 20 km/h (Fig. 1c). Both the ego vehicle and e-scooter were instrumented with high-accuracy real-time kinematic (RTK) GPS to measure position, heading, speed, and acceleration. Brake and throttle pedal signals were acquired from the vehicle's internal system. All signals were synchronized to 25 Hz.

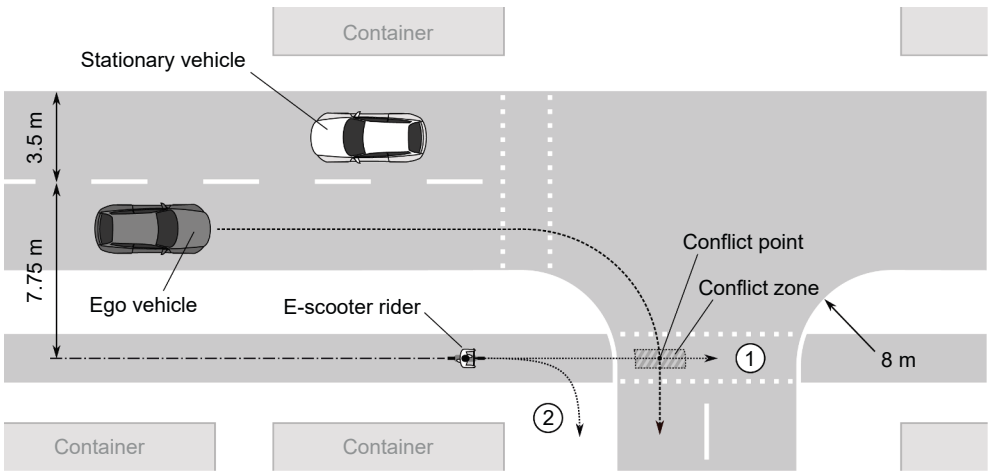

Fig. 2. The test-track scenario, illustrating the ego vehicle turning at the intersection and the two possible e-scooter travel directions: straight (1) and right (2).

2.1.3. Participants

Participants were employees of Magna Electronics recruited in Vårgårda due to the proximity to the test track. Their selection was based on these criteria: 1) held a valid driver's license, 2) drove a car at least three times a week, 3) did not drive as a profession, and 4) were between 18 and 60 years old. The experiment was approved by the Swedish Ethical Review Authority (Dnr 2023-03811-01). Twenty-five (seven female) participants, average age 42 years with a standard deviation (SD) of 11 years, took part in the experiment. On average, they drove seven times per week, mostly on rural roads, with an annual mileage of 10,000–20,000 km. All of them represented drivers within the Swedish population and none were directly involved in traffic safety research.

Out of all recorded data (250 runs, including baseline runs), nine runs had to be discarded due to missing or invalid data from the e-scooter. The remaining data (241 runs) contained three crashes in which the e-scooter crashed into the ego vehicle. These crashes occurred because the driver was expecting the e-scooter to slow down, but it did not. Because there were too few crashes for useful analysis, we removed them from the data used for modeling, thereby avoiding the possibility that they affected subsequent driver behavior.

2.2. Analyses and models

2.2.1. Interaction criticality

We measured interaction criticality by 1) post-encroachment time (PET) with respect to the conflict zone and 2) the ego vehicle speed at the moment it entered the zone. We calculated PET as the time elapsed between the rear end of the first vehicle leaving the conflict zone and the front of the second vehicle entering it (Allen et al., 1978). A PET closer to zero indicates a more critical interaction with a higher risk of a collision, as the road users miss each other with a smaller margin.

The PET may have been underestimated when the car entered the conflict zone first; in real life, the e-scooter rider could be expected to slow down to avoid a crash, unlike the e-scooter in our experiment which was not designed to change speeds. Therefore, to obtain a better measure of criticality for car-first maneuvers, we calculated the deceleration that would be required for the e-scooter to come to a full stop before entering the conflict zone ($dec_{req} = 0.5\ V^2_{scooter}/s_{scooter}$). This value was determined at the time when the car entered the conflict zone.

2.2.2. Statistical models

We modeled two critical aspects of driver behavior as the car approached the conflict zone (Fig. 2): 1) the *yielding decision*, and 2) the *braking* timing and intensity. For the models, we only used data from the trials in which the e-scooter traveled straight (the possible conflict interactions: 141 runs).

We used Bayesian regression to model driver behavior. Unlike frequentist regression, Bayesian regression relies on Bayes' theorem to calculate conditional probabilities using prior information and the specification of a model of the likelihood distribution (McElreath, 2020). Bayesian models facilitate interpreting results by representing the uncertainty in estimated quantities (for example, model parameters and predictions) with full probability distributions. All models were created in R (version 4.3.2) using *brms* (version 2.20.4), an R package for Bayesian regression via Markov chain Monte-Carlo (MCMC) sampling (Bürkner, 2017). For all models, we used non-informative prior distributions and four chains, each with 2000 iterations. The first 1000 were used for warmup and discarded, yielding 4000 MCMC samples in total. We checked the convergence of the MCMC algorithm using the default diagnostics included in brms and verified that the model generated distributions of observations similar to those in the data (by means of posterior-predictive checks; Gabry et al., 2019). We summarized the uncertainty in estimates with the 95 % highest-density interval (HDI; [lower bound, upper bound]) of posterior predictive distributions and the probability of direction (PD), defined as the probability that the posterior distribution has the sign of the median (Makowski et al., 2019).

For model development, we used the approximate leave-one-out cross-validation (LOOCV) implemented in brms, which computes the expected log-posterior density (ELPD), a measure of the predictive ability of a model (the greater, the better). To choose between model candidates, we assessed whether the improvement in ELPD was "clear" (i.e., greater by an order of magnitude than its estimation error). For a final model evaluation, we performed k-fold cross-validation grouped by individual drivers, with the model estimated on all but one driver—and predicted the response variable for the left-out driver (using 100 draws from the posterior predictive distributions). For binary model responses, we assessed performance with the area under the receiver-operating characteristic curve (AUC) and accuracy. In contrast, we used the root-mean-square error (RMSE) for numeric responses. The parameter distributions reported in the paper are based on the complete dataset (141 runs), to make full use of the data.

2.2.2.1. Yielding decision. We modeled the driver's decision to yield to the e-scooter with a Bayesian logistic regression, which models binary observations (driver yield/e-scooter first = 1, driver does not yield/car first = 0) as being sampled from a Bernoulli distribution. We obtained the best-performing model by using the predictors ego vehicle speed (V_{ego}) and difference in time-to-arrival (ΔTTA). Previous research has already found that both signals are important predictors of encroachment sequences in crossing scenarios (Mohammadi et al., 2025). To improve model convergence and allow comparisons between estimated parameters, we standardized V_{ego} and ΔTTA before model fitting by subtracting the mean and dividing by one SD. To account for variability among drivers, we included a "group-level effect" (similar in concept to a random effect in frequentist regression) on the intercept (Bürkner, 2017).

Equation (1) shows the yielding-decision model:

$$\begin{aligned} &\text{yield}_i \sim \text{Bernoulli}\ (p_i) \\ &\text{logit}\ (p_i) = \beta_0 + \beta_V V^s_{\text{ego},i} + \beta_{\Delta\text{TTA}} \Delta\text{TTA}^s_i + u_{\text{ID},i}, \\ &u_{\text{ID},i} \sim N(0, \sigma_{\text{ID}}) \end{aligned} \tag{1}$$

In Eq. (1), p_i represents the probability that the driver is yielding. V^s_{ego} and ΔTTA^s are the standardized predictors (denoted by superscript "s"), also referred to as "population-level effects" (Bürkner, 2017). The population-level parameters of the model are denoted by β, and the group-level effect on the intercept from an individual driver is denoted by u_{ID}, assumed to be sampled from a zero-centered normal distribution with SD σ_{ID}.

We calculated ΔTTA as the difference in TTAs between the e-scooter and the ego vehicle ($\Delta\text{TTA} = \text{TTA}_{\text{scooter}} - \text{TTA}_{\text{ego}}$). For the e-scooter, we estimated TTA as the time remaining before its arrival at the conflict point (the point within the conflict zone where the projected trajectories intersect; Fig. 3a), assuming a constant speed of 20 km/h. For the ego vehicle, we estimated TTA by taking into account the ego vehicle's projected speed as the driver braked for the approaching turn. We projected the speed using three different phases, based on how far the ego vehicle was from the conflict point (Fig. 3b): 1) a constant-speed phase until the moment at which the vehicle was predicted to start braking to arrive at the start of the turn at the assumed turning speed of 10 km/h while braking with an acceleration of -2 m/s^2, 2) a linear decrease in speed with the assumed braking acceleration, and finally 3) a constant turning speed of 10 km/h.

Both V_{ego} and ΔTTA were measured from the first decisive brake reaction by the driver to initiate the slowdown ahead of the turn, referred to in the following as *brake onset*. We thereby assumed that drivers decided to yield before they started to brake. To detect the brake onset, we examined the signals in the interval from the time the driver reached the intended speed until the driver started the turn (Fig. 4). Within this interval, we defined the last moment when the throttle-pedal deflection signal reached zero as the time when the driver released the pedal (*throttle release*). We then defined the brake onset as the first instance after the throttle release when the driver started pushing the brake pedal (obtained from the brake-pedal deflection signal).

2.2.2.2. Braking timing and intensity. We modeled both the timing and strength of drivers' braking with: 1) the TTA at brake onset and 2) the average deceleration between brake onset and brake release. Because of the physical correlation between the two measures, we modeled them jointly with a multivariate normal distribution. Since both measures are strictly positive, we log-transformed them. Then we standardized the responses to be able to compare estimated parameters between TTA and deceleration. We used the independent variables yielding decision and ego speed, and included variability between individual drivers through a group-level effect on the intercept.

Equation (2) shows the model with all its parameters, sampling timing (TTA) and strength (dec) from a multivariate normal distribution.

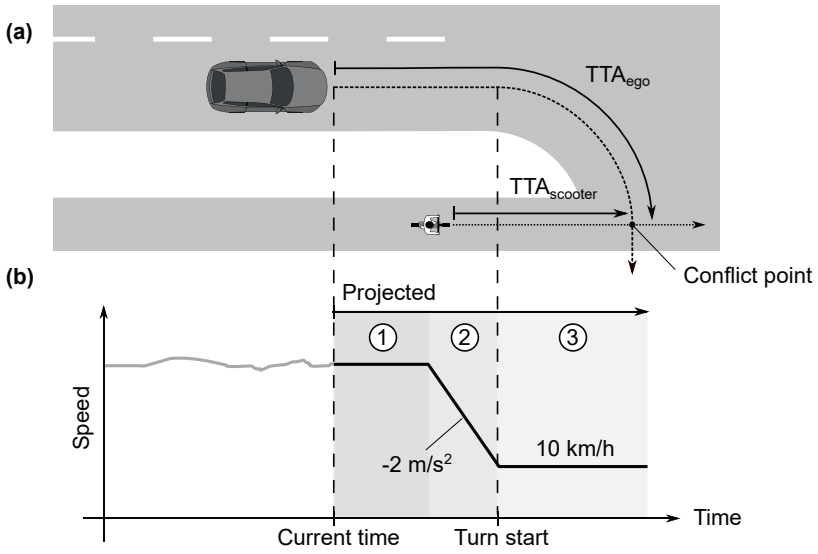

Fig. 3. Illustration of the curvilinear coordinate system (dotted lines with zero at the conflict point; panel a) and of the projected time-to-arrival of the ego vehicle (TTA_{ego}), based on its estimated speed profile (panel b). We estimated the speed profile as composed of three different phases: 1) constant speed, 2) linear speed decrease ahead of the turn, and 3) constant turning speed (panel b). The two vertical dashed lines mark the current time from which the speed of the ego vehicle is projected and the start of the turn, respectively.

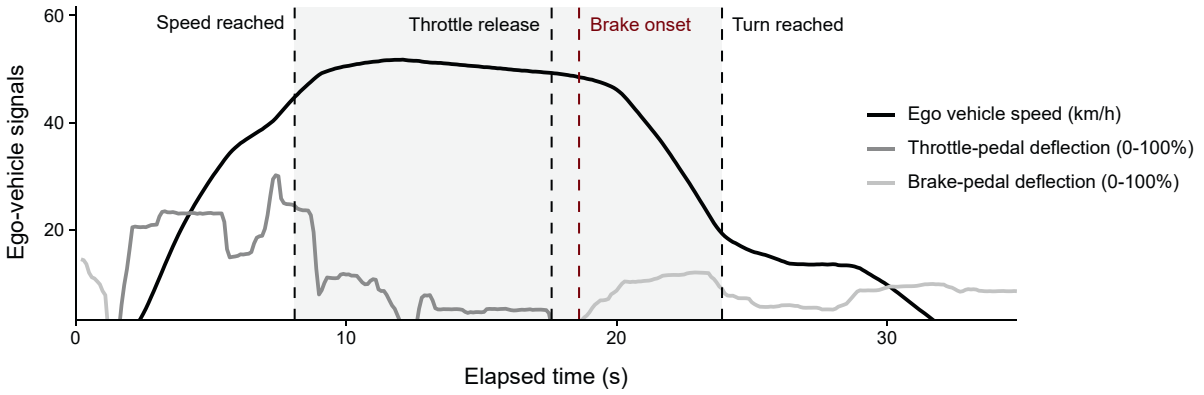

Fig. 4. Illustration of the detected times of interest for a typical yielding maneuver, indicated by vertical dashed lines: target-speed reached, throttle-pedal release, brake-pedal onset, and turn reached. The gray area marks the time interval considered for finding the throttle release and brake onset.

$$
\begin{aligned}
&\begin{pmatrix} \text{logTTA}_i^s \\ \text{logdec}_i^s \end{pmatrix} \sim \text{MVNormal}\left[\begin{pmatrix} \mu_{\text{TTA},i} \\ \mu_{\text{dec},i} \end{pmatrix}, \sum\right] \\
&\mu_{\text{TTA},i} = \beta_0^{\text{TTA}} + \beta_{\text{yield}}^{\text{TTA}}\text{yield}_i + \beta_V^{\text{TTA}} v_{\text{ego},i}^s + u_{\text{ID},i}^{\text{TTA}} \\
&\mu_{\text{dec},i} = \beta_0^{\text{dec}} + \beta_{\text{yield}}^{\text{dec}}\text{yield}_i + \beta_V^{\text{dec}} v_{\text{ego},i}^s + u_{\text{ID},i}^{\text{dec}} \\
&\sum = \begin{pmatrix} \sigma_{\text{TTA}} & 0 \\ 0 & \sigma_{\text{dec}} \end{pmatrix}\begin{pmatrix} 1 & \rho \\ \rho & 1 \end{pmatrix}\begin{pmatrix} \sigma_{\text{TTA}} & 0 \\ 0 & \sigma_{\text{dec}} \end{pmatrix}
\end{aligned}
\tag{2}
$$

In Eq. (2), σ_{TTA} and σ_{dec} are the residual SDs of the two response variables, and ρ represents their correlation. The group-level intercepts for individual drivers for TTA and dec are $u_{\text{ID},i}^{\text{TTA}}$ and $u_{\text{ID},i}^{\text{dec}}$, respectively, capturing the SDs ($\sigma_{\text{ID}}^{\text{TTA}}$ and $\sigma_{\text{ID}}^{\text{dec}}$) and the correlation across responses (ρ_{ID}) from a zero-centered multivariate normal distribution:

$$
\begin{aligned}
&\begin{pmatrix} u_{\text{ID},i}^{\text{TTA}} \\ u_{\text{ID},i}^{\text{dec}} \end{pmatrix} \sim \text{MVMormal}\left[\begin{pmatrix} 0 \\ 0 \end{pmatrix}, \mathbf{S}\right] \\
&\mathbf{S} = \begin{pmatrix} \sigma_{\text{ID}}^{\text{TTA}} & 0 \\ 0 & \sigma_{\text{ID}}^{\text{dec}} \end{pmatrix}\begin{pmatrix} 1 & \rho_{\text{ID}} \\ \rho_{\text{ID}} & 1 \end{pmatrix}\begin{pmatrix} \sigma_{\text{ID}}^{\text{TTA}} & 0 \\ 0 & \sigma_{\text{ID}}^{\text{dec}} \end{pmatrix}
\end{aligned}
\tag{3}
$$

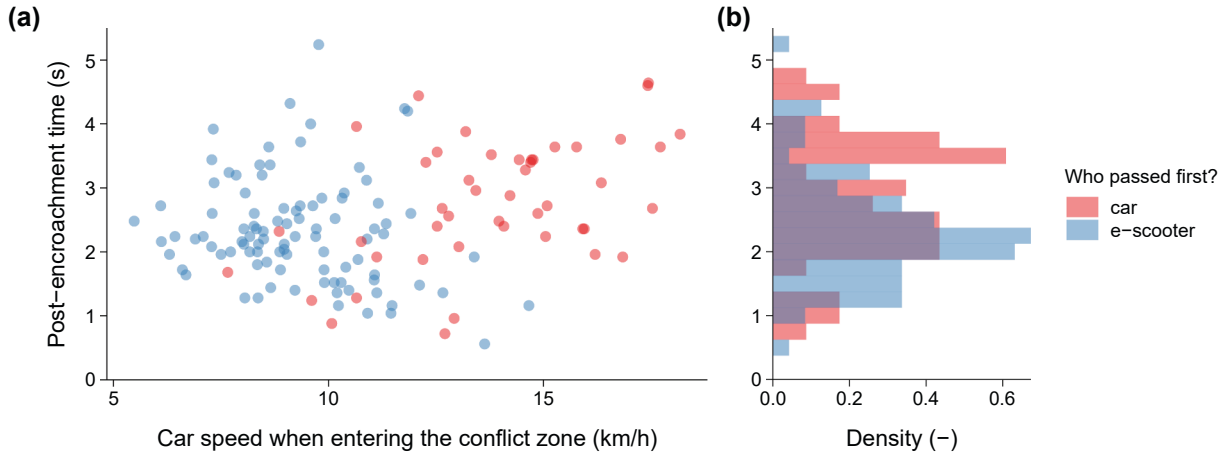

Fig. 5. Post-encroachment time between car and e-scooter and car speed when entering the conflict zone.

3. Results

3.1. Data overview and interaction criticality

In the 141 runs with the straight-traveling e-scooter used for modeling, drivers yielded 81.7 % of the time when approaching at 30 km/h, and 52.9 % of the time at 50 km/h. We observed differences between individual drivers in their tendency to yield: eight drivers yielded in all trials and one driver never yielded. PET values ranged from 0.56 s to 5.24 s (mean 2.47 s; SD 0.90 s; Fig. 5). For both yielding outcomes, we observed PET values close to zero, indicating critical interactions. Compared to the PETs for e-scooter-first maneuvers, those for car-first maneuvers appeared to peak around larger values (Fig. 5b), while the ego vehicle speed at the moment of entering the conflict zone was higher (Fig. 5a). Table 1 provides a summary of the variables used for analyses.

In car-first maneuvers, the e-scooter was on average 27.0 m (ranging from 15.3 to 37.7 m) away from the conflict zone when the driver entered it. Assuming braking with constant deceleration and a speed of 20 km/h, the required deceleration for the e-scooter to come to a complete stop before entering the conflict zone would have been 0.6 m/s^2 on average (min 0.4, max 1.0 m/s^2). These values are well below those reported by Li, Kovaceva, and Dozza (2023) for a small e-scooter's comfortable and harsh braking (1.65 and 2.92 m/s^2, respectively), as well as those for a large e-scooter such as those used by shared mobility services (1.98 and 4.04 m/s^2, respectively).

3.2. Yielding decision

The model agreed with the experimental data overall by predicting similar posterior distributions of the two yielding outcomes (Fig. 6a). The model parameters indicate that drivers were less likely to yield at higher approaching speeds and larger projected gaps with the e-scooter (with similar magnitudes of effect; Fig. 6b and 6c). In cross-validation, the model scored an AUC of 0.94 [0.91, 0.96] 95 % HDI and a median accuracy of 0.82 [0.75, 0.88] 95 % HDI. As a comparison, a dummy classifier that ignores any independent variables and always predicts yielding (the most common decision from the data) would have an accuracy of 0.67. The model parameters are summarized in Table 2. Adding the group-level effect for individual drivers improved the model (ELPD increased by 11.1, with a standard error of 4.9). Earlier model formulations included intrinsic driver parameters (e.g., gender, age, and yearly mileage) and interactions between speed and ΔTTA, but the effect on the model's predictive capabilities was not clear (ELPD score varied in the order of magnitude of its standard error).

3.3. Control

Compared to the 50 km/h trials, we observed an earlier divergence in ego vehicle speed between car-first maneuvers and e-scooter-first or baseline maneuvers in distance (Fig. 7a) and time (Fig. 8a) in the 30 km/h trials. Brake timing and acceleration appeared qualitatively similar over distance (Fig. 7b) for both speeds, while at 50 km/h, drivers generally braked earlier (Fig. 7a) and harder (Fig. 7b and 8b). They also braked earlier when yielding to the e-scooter than when not yielding or in baseline trials (Fig. 7a). In contrast to 30 km/h, at 50 km/h, drivers' speed profiles appeared very similar to baseline trials when passing first.

The braking model agreed with the experimental data, predicting similar posterior distributions of TTA and deceleration (Fig. 9a). The model parameters confirmed that drivers braked earlier and harder (in the same order of magnitude of effect) when approaching the intersection at the higher speed (Fig. 9b). In cross-validation, the model predicted TTA with an RMSE of 1.42 [1.23, 1.64] 95 % HDI s and deceleration with an RMSE of 0.33 [0.27, 0.39] 95 % HDI m/s^2. The model parameters are summarized in Table 3. Adding the group-level effect for individual drivers improved the braking model (ELPD increased by 26.5, with a standard error of 7.1). As for the yielding model, neither gender, age, yearly mileage, nor interactions between predictors improved its performance.

4. Discussion

We believe that our small test-track experiment managed to capture some of the differences between participants. This interpretation of our results is supported by the fact that most participants indicated in the post-drive survey that the environment was realistic,

Table 1
Data summary grouped by target speed and yielding decision (car first vs. e-scooter first), including number of runs (N). Variables are summarized as mean (SD).

Variable (unit)	Target speed 30 km/h		Target speed 50 km/h	
	Car first (N = 13)	E-scooter first (N = 58)	Car first (N = 33)	E-scooter first (N = 37)
Post-encroachment time (s)	2.62 (1.25)	2.38 (0.92)	2.85 (0.85)	2.21 (0.67)
V_{ego} when entering conflict zone (m/s)	3.81 (0.69)	2.65 (0.53)	3.86 (0.69)	2.47 (0.39)
Difference in TTA at brake onset ($\Delta TTA = TTA_{scooter} - TTA_{ego}$) (s)	2.07 (1.10)	0.18 (1.71)	1.92 (0.99)	0.75 (1.13)
V_{ego} at brake onset (m/s)	9.55 (0.98)	8.58 (0.88)	13.74 (0.76)	13.63 (0.78)
TTA_{ego} at brake onset (s)	9.38 (1.28)	9.70 (1.27)	10.40 (1.40)	12.11 (1.59)
Mean deceleration during braking (m/s^2)	1.01 (0.28)	0.92 (0.28)	1.56 (0.30)	1.26 (0.29)

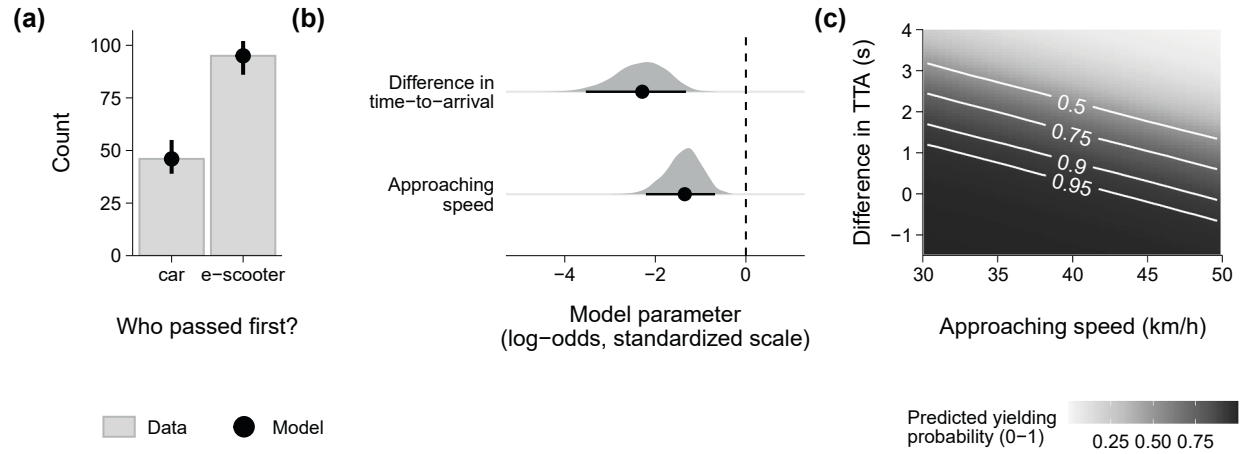

Fig. 6. Yielding-decision model predictions vs. data (panel a), the fitted model parameters on a standardized scale (panel b), and predictions of the model across the two independent variables (panel c). The black dots and error bars represent the median and 95% highest-density interval, respectively, of the posterior distribution of the model responses (panel a) and parameters (panel b). The predicted yielding probability shown in panel c (with some levels annotated) is calculated without the group-level effect of individual drivers.

Table 2
Parameters of the yielding-decision model, summarized with median, lower and upper limit of the 95 % highest-density interval (HDI), and probability of direction (PD; Makowski et al., 2019). To predict model responses to new data, the independent variables ego vehicle speed (V) and difference in time-to-arrival (ΔTTA) must first be standardized by subtracting the original data means (11.20 m/s and 0.91 s, respectively) and then divided by the SD (2.62 m/s and 1.56 s, respectively).

Parameter	Median	l-95 % HDI	u-95 % HDI	PD
β_0	1.95	0.90	3.30	1.00
$\beta_{\Delta TTA}$	−2.29	−3.44	−1.25	1.00
β_V	−1.35	−2.16	−0.65	1.00
σ_{ID}	2.09	1.04	3.53	1.00

suggesting that they behaved as they usually would have (Fig. A.1 in Appendix A). The models we developed, despite using static data as opposed to the full time series, captured key aspects of the right-turn maneuver: the initial decision-making (to yield or not to yield) and the execution of the braking (timing and strength).

Our results indicate that drivers appear to possibly behave more riskily at higher speeds, yielding less often to the e-scooter when they have less time to assess the e-scooter's position. When passing first, drivers maintained higher speeds through the conflict zone; while this may incur an increased injury potential in case of a collision, it also frees up the intersection for the approaching e-scooter. Furthermore, at the higher speed, drivers braked not only earlier but also harder, which suggests that those maneuvers were indeed riskier. These findings may support decreasing speed around intersections where drivers need to interact with e-scooter riders. Given that Pérez-Zuriaga et al. (2023) showed that, at higher speeds, e-scooter riders are more vulnerable to motorized vehicles than cyclists are, this change could be particularly significant for improving the safety of e-scooter riders.

Infrastructure design should assess measures to improve drivers' decision-making. For instance, redesigned intersections could increase the visibility of the e-scooter (Deliali et al., 2021), allowing drivers to assess the need to yield earlier and plan their slowdown accordingly. Infrastructure may also employ smart sensors that can sense movement, predict collision risk, and warn both drivers and e-scooter riders when needed (Saul et al., 2021). The system's decision to activate could be guided by assessessing whether the actual driver behavior deviates from the reference behavior predicted by our models.

Driving style, whether cautious or assertive, appeared to be intrinsic, at least for some drivers. For instance, some drivers never yielded while others always yielded, regardless of the situation. The decision to yield may be linked to driver characteristics such as proneness to risk-taking (Taubman-Ben-Ari & Yehiel, 2012). While predicting driving style was neither directly part of this study nor incorporated into the model, the model does incorporate at least part of this intrinsic behavior: the group-level effect captures some variability due to the specific participant.

Drivers appeared to be influenced by the e-scooter, particularly its positioning and the projected gap at the conflict point—indicating that they were aware of the e-scooter and able to project its movement to some extent. We found driver behavior in the car-first trials very similar to that in the baseline trials with a stationary e-scooter, perhaps indicating that when drivers have decided to pass first, they are not concerned anymore about the e-scooter, and simply brake as usual when turning. This behavior may be a result of the legislation described previously which requires e-scooter riders to give way at unsupervised bicycle passages (Swedish Transport Agency, 2016).

The models are a reference for driver behavior when interacting with an e-scooter at an intersection. This reference could be used to

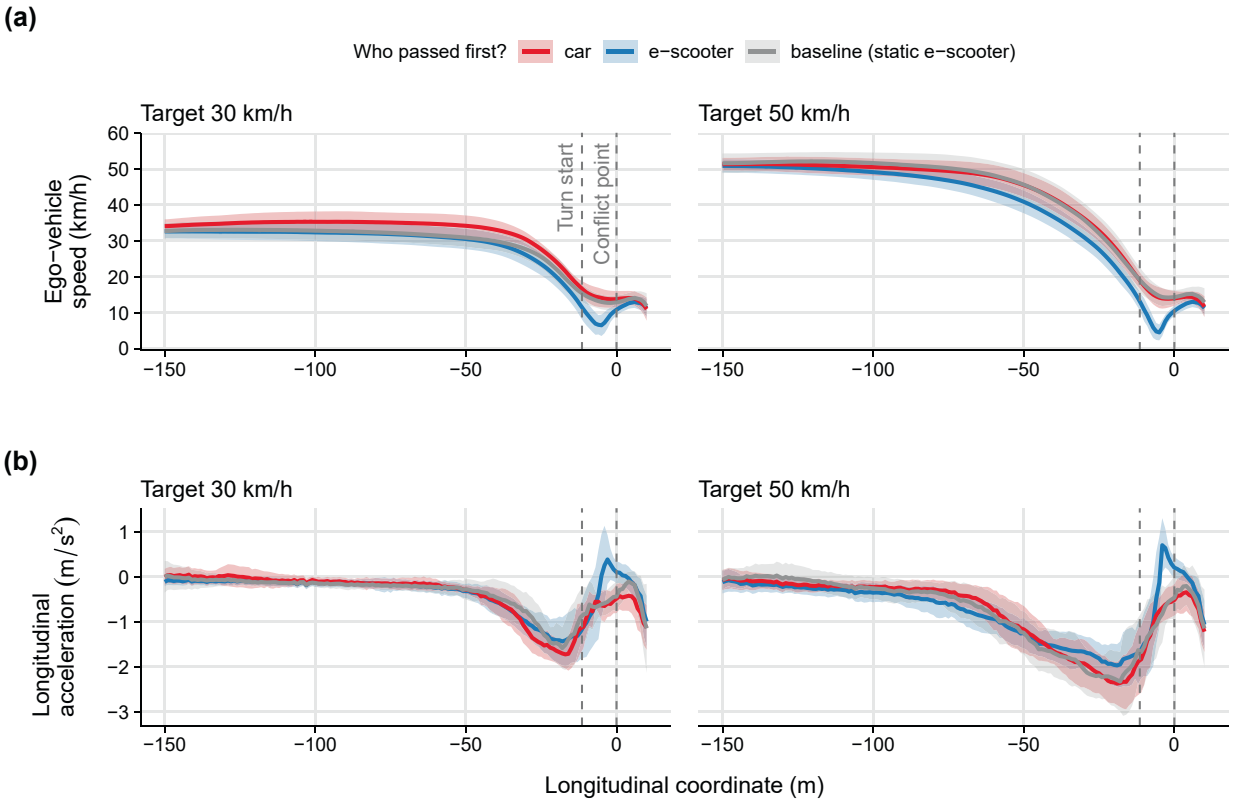

Fig. 7. Ego vehicle speed (upper panels) and acceleration (lower panels). The solid lines represent the mean and the ribbons represent +/-1 SD. The x-axis shows the longitudinal coordinate of the curvilinear coordinate system that follows the right turn (see Fig. 3 for an illustration). The vertical dotted lines mark the coordinates of the start of the turn and the conflict point.

inform the design of ADAS. For instance, the models could be used to tune system warnings and interventions, based on the probability of a driver yielding to the e-scooter and the way an individual driver would brake in specific circumstances. The tuning could prevent activations perceived as false positives by the driver (Lubbe & Rosén, 2014). For example, if the ADAS registers that a driver has not yet braked to yield, but the model predicts a high yielding probability, it could trigger a warning to ensure that the driver is aware of an approaching e-scooter. Otherwise, the warning could be suppressed to reduce annoyance. Similarly, vehicle safety systems could be adapted to the predicted brake timing and intensity, providing additional support if the braking applied is insufficient to ensure the e-scooter's safe passage. The fact that individual drivers appear to differ in their tendency to yield (as incorporated through the group-level effect in our models) suggests that ADASs may become more effective if they are adapted to the individual driver.

Our results and models may also be useful for organizations such as Euro NCAP, since they can inform the testing and assessment procedure to promote safer vehicles. To ensure a safer right turn, a blind-spot support system might help drivers be more aware of the e-scooter's position, warning the driver when the e-scooter is approaching from behind and the driver appears to be passing first. (In fact, most participants indicated that the blind spot was a safety issue.) An autonomous emergency braking (AEB) system could serve as a backup solution, slowing down the vehicle if the driver does not react to the warning (Stigson et al., 2024). Euro NCAP currently tests AEB systems for near-side turning cars, with pedestrians approaching from both opposite and same directions, but with *cyclists* approaching only from the *opposite* direction (Euro NCAP, 2023). Future assessment may, therefore, consider including blind-spot support systems that *warn* the driver or slow down the vehicle in scenarios where any type of VRU (including cyclists and e-scooter riders) is approaching in the *same* direction as the vehicle. Similar systems were recently introduced for truck-to-cyclist AEB test scenarios (Euro NCAP, 2024). The computational models could also improve the ecological validity of virtual testing by simulating reference values for average drivers while also including personal variability.

Prior research has studied drivers' right-turn interactions with cyclists, while e-scooters have not yet garnered the same attention. A direct comparison of drivers' responses to e-scooter riders vs. cyclists was not in the scope of this study. However, in light of previous studies with cyclists, we can offer some reflections on potential differences. E-scooters and bicycles likely appear visually different to drivers, at far and near distances, despite possibly using the same infrastructure (e.g., cycle path). However, our current findings do not suggest any obvious differences in driver behavior. For instance, drivers adapt their kinematic behavior in response to their own speed and the cyclist's kinematics (Schindler & Bianchi Piccinini, 2021; Silvano et al., 2016), suggesting that what we have learned from cyclists can be transferred at least partially to e-scooters. While cyclist research has extensively investigated drivers' glance behavior in interactions with cyclists (Denk et al., 2023; Jansen & Varotto, 2022; Kircher et al., 2020; Schindler & Bianchi Piccinini, 2021), glance

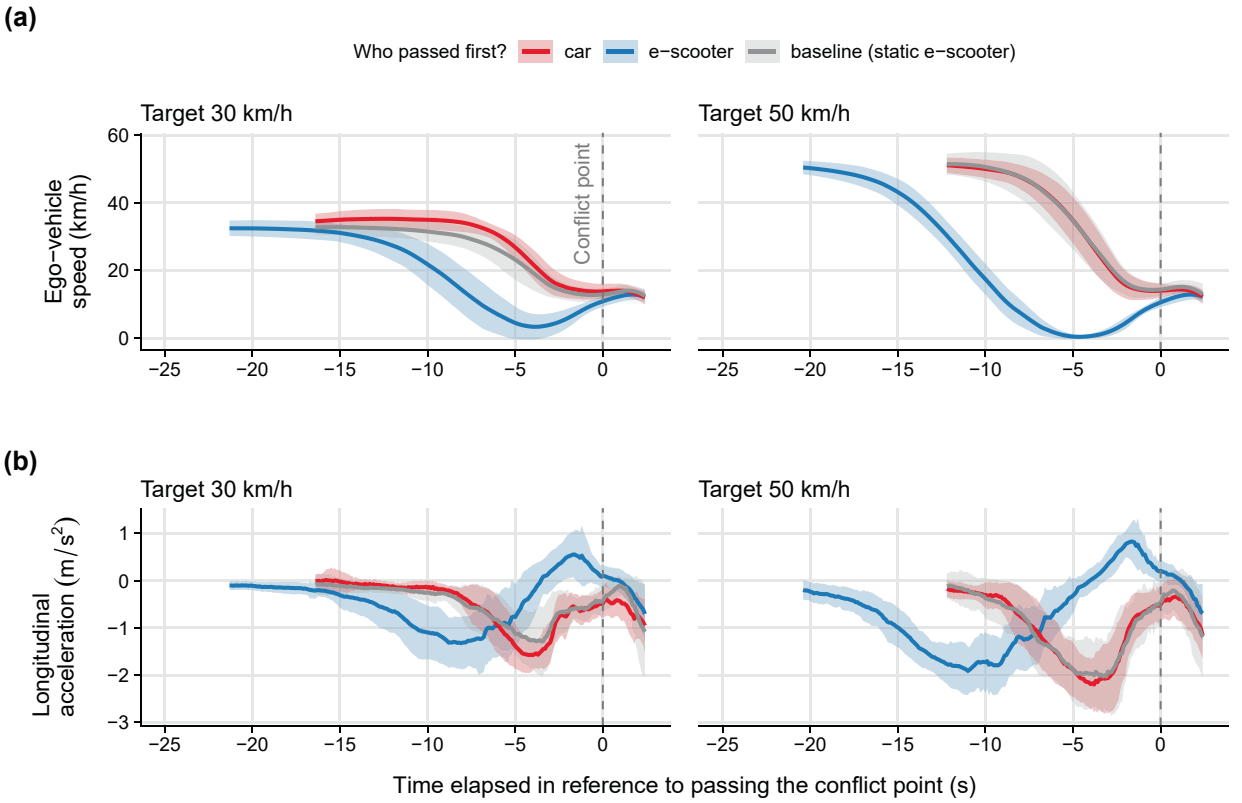

Fig. 8. Ego vehicle speed (upper panels) and acceleration (lower panels). The solid lines represent the mean and the ribbon +/-1 SD. The x-axis shows the time elapsed relative to the geometrical center of the ego vehicle passing the conflict point (Fig. 3). The vertical dotted line marks the moment of arriving at the conflict point.

behavior was beyond the scope of this study. Future work may assess drivers' glance behavior in e-scooter interactions in order to determine if there are significant differences, or to possibly further improve ADASs.

The generalizability of our results is limited by the subset of the driving population who participated in the experiment. Due to the location of the test track, participants were more used to driving on rural roads than an urban population would be; therefore, they may have been less used to interacting with e-scooter riders and might have reacted more cautiously, compared to urban drivers. The generalizability of the results may be further limited by differences in regulations about cycle passages between Sweden and other countries. Furthermore, our study represents only one example of a bicycle passage with a specific geometry. While our definition of TTA can be adapted to different turns (by adjusting the assumed speed profile of the driver) and the observed driver behavior is similar to that in previous studies with cyclists (Silvano et al., 2016), the extent of generalizability to other passages may need to be assessed in future work.

Because the robot that controlled the e-scooter was not designed to adjust its speed in response to the car, some interactions might have been less natural. Some drivers may have expected it to slow down when entering the intersection, as both driver and rider share responsibility for safe interactions (Swedish Transport Agency, 2016). Consequently, our results may be biased toward more conservative driver behaviors. However, we do not yet know how e-scooter riders behave in real-world interactions with drivers. Future work should, therefore, aim to understand rider behavior in similar, real-world scenarios—through data from field tests or naturalistic studies, for instance (Pai & Dozza, 2025). Understanding and modeling when and how riders choose to slow down may help predict and prevent dangerous interactions, for instance, when riders unexpectedly choose not to slow down and risk a close encounter with the car. With (ideally) naturalistic data and more sophisticated time series models, including game theory (Mohammadi et al., 2025), future work should develop models that capture more of the dynamics of these interactions.

5. Conclusion

We investigated how drivers negotiate a right turn at an intersection in the presence of an e-scooter. Drivers yielded less often at higher speeds despite having less time to make an informed decision, highlighting the need to support drivers in these scenarios. Our computational models can provide a reference for driver behavior, supporting the design and testing of ADAS and higher forms of vehicle automation, thereby improving the safety of interactions between cars and e-scooters as well as user acceptance of the systems.

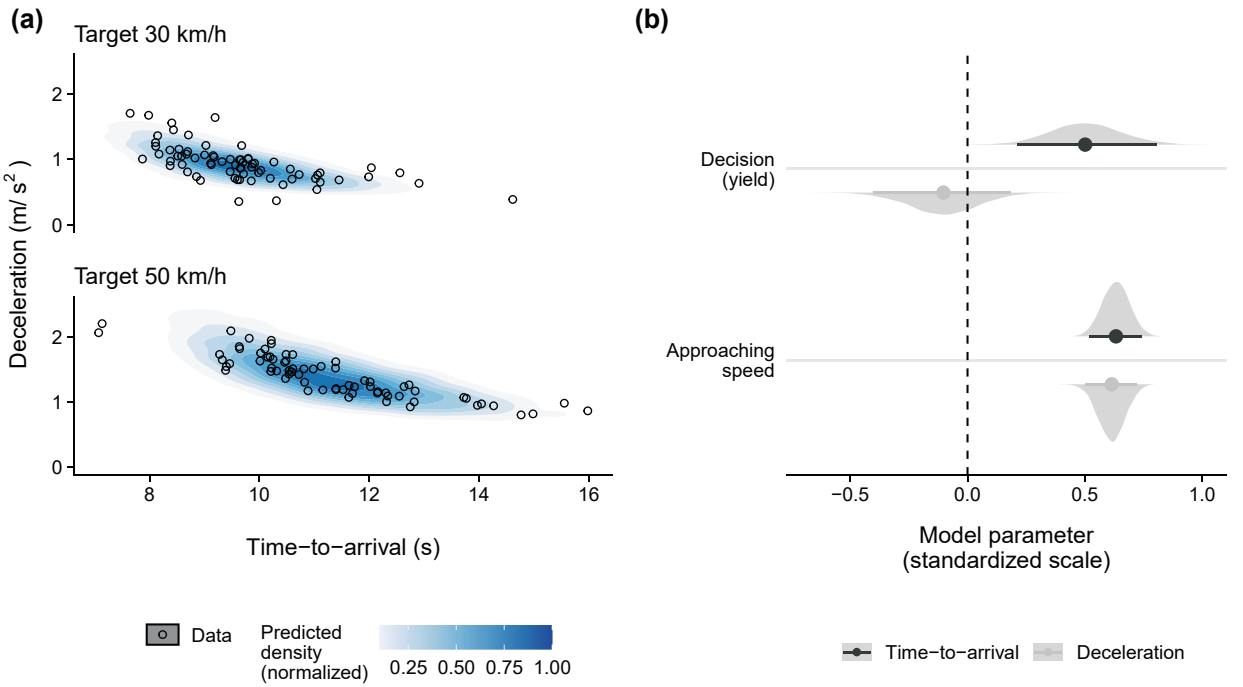

Fig. 9. Braking model fit (panel a) and fitted model parameters (panel b). The model predictions in panel a are shown as normalized 2D density over time-to-arrival and deceleration.

Table 3
Parameters of the braking model (combining time-to-arrival, TTA, and deceleration, dec), summarized with median, lower, and upper limits of the 95% highest-density interval (HDI) and probability of direction (PD; Makowski et al., 2019). To predict model responses to new data, the independent variable ego vehicle speed (V) must first be standardized (see Table 2 caption). The predicted response variables (TTA and dec, predicted on the standardized log scale) can be reverted from the standardized scale to their original scale by multiplying them by the original log-transformed data SDs (0.16 log s and 0.35 log m/s^2 for TTA and dec, respectively) and adding their means (2.34 log s and 0.10 log m/s^2 for TTA and dec, respectively), followed by reverting the log-transformation with the exponential function.

Parameter	Median	l-95 % HDI	u-95 % HDI	PD
β_0^{TTA}	0.07	−0.24	0.38	0.68
β_V^{TTA}	0.61	0.51	0.73	1.00
β_{yield}^{TTA}	−0.10	−0.42	0.17	0.76
β_0^{dec}	−0.34	−0.66	−0.04	0.98
β_V^{dec}	0.63	0.52	0.74	1.00
β_{yield}^{dec}	0.50	0.21	0.80	1.00
ρ_{ID}	−0.99	−1.00	−0.96	1.00
ρ	−0.82	−0.87	−0.75	1.00
σ_{ID}^{dec}	0.51	0.34	0.72	1.00
σ_{ID}^{TTA}	0.51	0.33	0.72	1.00
σ_{dec}	0.58	0.50	0.65	1.00
σ_{TTA}	0.59	0.52	0.68	1.00

CRediT authorship contribution statement

Alexander Rasch: Writing – review & editing, Writing – original draft, Visualization, Software, Methodology, Investigation, Formal analysis, Data curation, Conceptualization. **Alberto Morando:** Writing – review & editing, Writing – original draft, Software, Methodology, Data curation. **Prateek Thalya:** Writing – review & editing, Writing – original draft, Methodology, Investigation, Data curation, Conceptualization.

Declaration of Competing Interest

The authors declare the following financial interests/personal relationships which may be considered as potential competing interests: [A. Morando is employed at Autoliv (https://www.autoliv.com), a company that develops, manufactures, and sells protective

systems as well as mobility safety solutions. P. Thalya was employed at Magna Electronics (https://www.magna.com), a company that provides leading technologies for automated driving.].

Acknowledgments

The authors would like to thank the team at Magna Research for supporting the test-track experiment. We would further like to thank Marco Dozza (Chalmers) and Christian-Nils Åkerberg Boda (Autoliv) for valuable discussions related to the experiment and analyses, and Kristina Mayberry for language revisions.

This work has been carried out as part of the project e-SAFER, funded by VINNOVA (Sweden's innovation agency), the Swedish Transport Administration, the Swedish Energy Agency, and industrial partners within the FFI program under grant number 2022-01641.

Appendix A

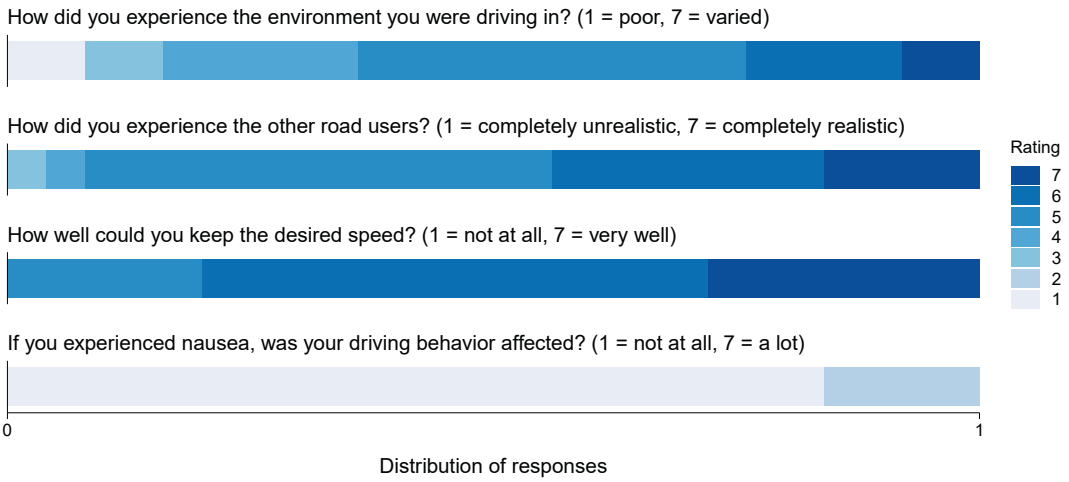

Fig. A1. Post-drive survey results, shown as the distribution of Likert-item scores indicated by drivers who participated in the experiment.

Data availability

The authors do not have permission to share data.

References

Agúndez, A. G., García-Vallejo, D., & Freire, E. (2024). An electric kickscooter multibody model: Equations of motion and linear stability analysis. *Multibody System Dynamics, 62*(4), 493–524. https://doi.org/10.1007/s11044-024-09974-4

Allen, B. L., Shin, B. T., & Cooper, P. (1978). Analysis of Traffic Conflicts and Collisions. *Transportation Research Record, 667*, 67–74.

Brännström, M., Coelingh, E., & Sjöberg, J. (2010). Model-based threat assessment for avoiding arbitrary vehicle collisions. *IEEE Transactions on Intelligent Transportation Systems, 11*(3), 658–669. https://doi.org/10.1109/TITS.2010.2048314

Bürkner, P.-C. (2017). brms : An R Package for Bayesian Multilevel Models using Stan. *Journal of Statistical Software, 80*(1). https://doi.org/10.18637/jss.v080.i01

Clough, R. A., Platt, E., Cole, E., Wilson, M., & Aylwin, C. (2023). Major trauma among E-Scooter and bicycle users: A nationwide cohort study. *Injury Prevention, 29*(2), 121–125. https://doi.org/10.1136/ip-2022-044722

Deliali, K., Christofa, E., & Knodler, M. (2021). The role of protected intersections in improving bicycle safety and driver right-turning behavior. *Accident Analysis and Prevention, 159*(January), Article 106295. https://doi.org/10.1016/j.aap.2021.106295

Denk, F., Fröhling, F., Brunner, P., Huber, W., Margreiter, M., Bogenberger, K., & Kates, R. (2023). Design of an Experiment to Pinpoint Cognitive Failure Processes in the Interaction of Motorists and Vulnerable Road Users. 2023 IEEE Intelligent Vehicles Symposium (IV), 01, 1–8. doi:10.1109/IV55152.2023.10186550.

Distefano, N., Leonardi, S., Kieć, M., & D'Agostino, C. (2024). Comparison of E-Scooter and Bike users' Behavior in mixed Traffic. *Transportation Research Record*. https://doi.org/10.1177/03611981241263339

Euro NCAP. (2023). European New Car Assessment Programme (Euro NCAP) - Test Protocol AEB/LSS VRU Systems Version 4.4. In European New Car Assessment Programme. https://cdn.euroncap.com/media/77299/euro-ncap-aeb-lss-vru-test-protocol-v44.pdf.

Euro NCAP. (2024). Collision Avoidance Frontal Collisions Truck-to-Vulnerable Road User - Test Protocol. Euro NCAP. https://www.euroncap.com/media/80738/euro-ncap-trucks-ca-frontal-collisions-vru-test-protocol-v10.pdf.

Gabry, J., Simpson, D., Vehtari, A., Betancourt, M., & Gelman, A. (2019). Visualization in Bayesian workflow. *Journal of the Royal Statistical Society: Series A (Statistics in Society), 182*(2), 389–402. https://doi.org/10.1111/rssa.12378

Jansen, R. J., & Varotto, S. F. (2022). Caught in the blind spot of a truck : A choice model on driver glance behavior towards cyclists at intersections. *Accident Analysis and Prevention, 174*(July), Article 106759. https://doi.org/10.1016/j.aap.2022.106759

Kircher, K., Ahlström, C., Ihlström, J., Ljokkoi, T., & Culshaw, J. (2020). Effects of training on truck drivers' interaction with cyclists in a right turn. *Cognition, Technology and Work, 22*(4), 745–757. https://doi.org/10.1007/s10111-020-00628-x

Kovaceva, J., Bärgman, J., & Dozza, M. (2022). On the importance of driver models for the development and assessment of active safety: A new collision warning system to make overtaking cyclists safer. *Accident Analysis & Prevention, 165*(November 2021). https://doi.org/10.1016/j.aap.2021.106513

Hong, Y., Klauer, C., & Vilela, J. P. T. (2022). An Evaluation of Road User Interactions with E-Scooters.

Ljung Aust, M., & Dombrovski, S. (2013). Understanding and Improving Driver Compliance With Safety System. The 23th International Technical Conference on the Enhanced Safety of Vehicles (ESV).

Li, T., Kovaceva, J., & Dozza, M. (2023). Modeling Collision Avoidance Maneuvers for Micromobility Vehicles. *Journal of Safety Research, 87*, 232–243. https://doi.org/10.1016/j.jsr.2023.09.019

Lubbe, N., & Rosén, E. (2014). Pedestrian crossing situations: Quantification of comfort boundaries to guide intervention timing. *Accident Analysis and Prevention*. https://doi.org/10.1016/j.aap.2014.05.029

Lübbe, N. (2015). Integrated Pedestrian Safety Assessment: A Method to Evaluate Combinations of Active and Passive Safety.

Makowski, D., Ben-Shachar, M. S., Chen, S. H. A., & Lüdecke, D. (2019). Indices of effect Existence and significance in the Bayesian Framework. *Frontiers in Psychology, 10*(December), 1–14. https://doi.org/10.3389/fpsyg.2019.02767

McElreath, R. (2020). *Statistical Rethinking: A Bayesian Course with examples in R and Stan* (2nd ed.). Chapman and Hall/CRC, 10.1201/9780429029608.

Mohammadi, A., Kalantari, A. H., Markkula, G., & Dozza, M. (2025). Cyclists' interactions with professional and non-professional drivers: Observations and game theoretic models. *Transportation Research Part F: Traffic Psychology and Behaviour, 112*(August 2024), 48–62. https://doi.org/10.1016/j.trf.2025.03.026

Pai, R. R., & Dozza, M. (2025). Understanding factors influencing e-scooterist crash risk: A naturalistic study of rental e-scooters in an urban area. *Accident Analysis and Prevention, 209*(June 2024). https://doi.org/10.1016/j.aap.2024.107839

Pérez-Zuriaga, A. M., Dols, J., Nespereira, M., García, A., & Sajurjo-de-No, A. (2023). Analysis of the consequences of car to micromobility user side impact crashes. *Journal of Safety Research, 87*, 168–175. https://doi.org/10.1016/j.jsr.2023.09.014

Saul, H., Junghans, M., Dotzauer, M., & Gimm, K. (2021). Online risk estimation of critical and non-critical interactions between right-turning motorists and crossing cyclists by a decision tree. *Accident Analysis and Prevention, 163*(January), Article 106449. https://doi.org/10.1016/j.aap.2021.106449

Schindler, R., & Bianchi Piccinini, G. (2021). Truck drivers' behavior in encounters with vulnerable road users at intersections: Results from a test-track experiment. *Accident Analysis & Prevention, 159*(May), Article 106289. https://doi.org/10.1016/j.aap.2021.106289

Schram, R., Williams, A., Ratingen, M. van, Ryrberg, S., & Sferco, R. (2015). Euro NCAP's first step to assess Autonomous Emergency Braking (AEB) for Vulnerable Road Users. The 24th International Technical Conference on the Enhanced Safety of Vehicles (ESV), 1–7.

Shah, N. R., Aryal, S., Wen, Y., & Cherry, C. R. (2021). Comparison of motor vehicle-involved e-scooter and bicycle crashes using standardized crash typology. *Journal of Safety Research, 77*, 217–228. https://doi.org/10.1016/j.jsr.2021.03.005

Sjöberg, J., Coelingh, E., Ali, M., Brännström, M., & Falcone, P. (2010). Driver models to increase the potential of automotive active safety functions. 18th European Signal Processing Conference (EUSIPCO-2010), 204–208.

Stigson, H., Kullgren, A., & Lubbe, N. (2024). Descriptive Statistics on Crashes of E-Scooters with Passenger Cars in Sweden. IRCOBI Conference 2024, 934–935. https://www.ircobi.org/wordpress/downloads/irc24/pdf-files/24122.pdf.

Silvano, A. P., Koutsopoulos, H. N., & Ma, X. (2016). Analysis of vehicle-bicycle interactions at unsignalized crossings: A probabilistic approach and application. *Accident Analysis & Prevention, 97*, 38–48. https://doi.org/10.1016/j.aap.2016.08.016

Statistisches Bundesamt. (2022). *Die neue Zweirad-Mobilität: Zum Unfallgeschehen mit Pedelecs und E-Scootern*. https://www.destatis.de/DE/Presse/Pressekonferenzen/2022/unfallgeschehen_pedelec_e-scooter/statement-pedelec_e-scooter.pdf.

Stray, A. V., Siverts, H., Melhuus, K., Enger, M., Galteland, P., Næss, I., Helseth, E., & Ramm-Pettersen, J. (2022). Characteristics of Electric Scooter and Bicycle Injuries after Introduction of Electric Scooter Rentals in Oslo, Norway. *JAMA Network Open, 5*(8), Article e2226701. https://doi.org/10.1001/jamanetworkopen.2022.26701

Swedish Transport Agency (2016). Bicycle passages and bicycle crossings (TS 201618). Blomquist & Co. https://www.transportstyrelsen.se/globalassets/global/publikationer-och-rapporter/vag/trafikant/produkter/tran-049-bicycle-passages-and-bicycle-crossings_a5_webb.pdf.

Taubman-Ben-Ari, O., & Yehiel, D. (2012). Driving styles and their associations with personality and motivation. *Accident Analysis and Prevention, 45*, 416–422. https://doi.org/10.1016/j.aap.2011.08.007

Wallhagen, S. (2023). Elsparkcyklar: Genomgång av internationell litteratur och analys av svenska olycksdata. https://vti.diva-portal.org/smash/get/diva2:1822411/FULLTEXT01.pdf.